A Journal of the Gesellschaft Deutscher Chemiker

Angewandte International Edition GDCh Chemie

www.angewandte.org

Accepted Article

Title: Mixed Metal-Organic Framework with Multiple Binding Sites for E fficient C2H2/CO2 Separation

Authors: Banglin Chen, Junkuo Gao, Xuefeng Qian, Ruibiao Lin, Rajamani Krishna, Hui Wu, and Wei Zhou

To be cited as: *Angew. Chem. Int. Ed.* 10.1002/anie.202000323
Angew. Chem. 10.1002/ange.202000323

Link to VoR: http://dx.doi.org/10.1002/anie.202000323
http://dx.doi.org/10.1002/ange.202000323

WILEY-VCH

10.1002/anie.202000323

WILEY-VCH

COMMUNICATION

Mixed Metal-Organic Framework with Multiple Binding Sites for Efficient C_2H_2/CO_2 Separation

Junkuo Gao,* Xuefeng Qian, Rui-Biao Lin,* Rajamani Krishna, Hui Wu, Wei Zhou,* Banglin Chen*

Abstract: The C_2H_2/CO_2 separation is particularly challenging owing to their high similarity in physical properties and molecular sizes, but of industrial significance. Herein we report a mixed metal-organic framework (M'MOF) [Fe(pyz)Ni(CN)$_4$] (**FeNi-M'MOF**, pyz = pyrazine) with multiple functional sites and compact one-dimensional channels of ~4.0 Å for challenging C_2H_2/CO_2 separation. This MOF shows not only a remarkable volumetric C_2H_2 uptake of 133 cm^3 cm^{-3} but also an excellent C_2H_2/CO_2 selectivity of 24 under ambient condition, resulting in the second highest C_2H_2-captured amount of 4.54 mol L^{-1} that outperforms most previous benchmark materials. The separation performance of this material has been validated by dynamic breakthrough and neutron diffraction experiments, which is driven by π-π stacking and multiple intermolecular interactions between C_2H_2 molecules and the binding sites of **FeNi-M'MOF**. Besides, this material can be facilely synthesized by mixing method at room temperature and is water stable, jointly highlighting **FeNi-M'MOF** as a promising material for C_2H_2/CO_2 separation.

Metal-organic frameworks (MOFs) have emerged as very promising porous materials for adsorptive gas separation because they integrate the merits of tunable pore sizes and functional pore surface that can realize not only molecular sieving effect but also preferential gas binding.[1] Plenty of MOFs have been explored for simplifying various gas separation and purification schemes, ranging from mature ones such as carbon dioxide capture (CO_2) from methane and nitrogen to more challenging olefin/paraffin and alkyne/alkene separations.[2] For C_2H_2 and CO_2 gas molecules, their very high similarity in physical properties (differ in boiling point by ~3% and ~6 K), and identical molecular shapes/sizes (3.3 × 3.3 × 5.7 Å^3 for C_2H_2, 3.2 × 3.3 × 5.4 Å^3 for CO_2) with both kinetic diameters of ~3.3 Å, make it very difficult and challenging to realize efficient porous materials for C_2H_2/CO_2 separation under ambient conditions.[3] A few ultramicroporous MOFs featuring bare oxygen or fluorine base sites have been developed to preferentially bind C_2H_2 molecules through H-bonding interactions or bind CO_2 molecules through electrostatic interactions, showing high C_2H_2/CO_2 selectivity but low C_2H_2 uptake.[4] Another approach is to incorporate strong adsorption binding sites mainly open metal sites into MOFs with large pore volumes to boost the uptake capacity of the preferred gas molecules.[5] **UTSA-74** represents a unique example with open metal centers of two accessible sites, which can bind two C_2H_2 but one CO_2 molecules, differing from its isomer **MOF-74** which adsorbs similar amounts of C_2H_2 and CO_2 under the same condition.[5c] Though progresses have been made over the past several years, the uptake capacity versus selectivity trade-off still poses a daunting challenge for addressing C_2H_2/CO_2 separation.[6]

The vast database of reported MOF structures enables comparative analyses to target potential candidates with dual functionalities, featuring moderate pore volumes and accessible functional sites, to realize both high gas uptake and separation selectivities. Among plentiful ligands, cyanide is a short and highly basic ligand that is feasible to construct robust MOFs with modest pore aperture size, such as Prussian blue and Hofmann-type compounds.[7] For those MOFs with metalloligands, the open metal sites on ligands are accessible for gas molecules, whereas expected narrow pore structures originating from compact ligands enforce additional multiple intermolecular interactions to form, as demonstrated by a series of mixed metal-organic frameworks (M'MOFs).[8] In this regard, a Hofmann-type MOF [Fe(pyz)Ni(CN)$_4$] (**FeNi-M'MOF**, pyz = pyrazine) discovered in 2001, showing open nickel sites and polarized surfaces as well as compact pore channels of ~4.0 Å, is particularly interesting.[9] The high density of functional sites and ultramicropore would collaboratively enforce gas separation with high gas uptake and separation selectivities. Herein we investigate the mixed iron/nickel MOF **FeNi-M'MOF** for potential C_2H_2/CO_2 separation. In this MOF, C_2H_2 molecules are found to preferentially bind onto the organic moieties and open Ni sites through π-π stacking and multiple intermolecular interactions, respectively, whereas CO_2 molecules mainly distribute on the open Ni sites through relatively weak interactions. In this context, **FeNi-M'MOF** shows a very high C_2H_2/CO_2 selectivity of 24 that is superior to the previous top-performing MOFs while retaining a remarkable C_2H_2 uptake capacity of 133 cm^3 cm^{-3}, and thus an excellent C_2H_2-captured capacity of 4.54 mol L^{-1} at 298 K and 1 bar for 50:50 C_2H_2/CO_2 separation, which is close to that of the benchmark UTSA-74 and exceeds those of other out-performing MOFs.[5c]

FeNi-M'MOF is a pillared-layer M'MOF, in which the Fe[Ni(CN)$_4$] layer is connected by the pyz pillars. The Ni atoms show square-planar coordination geometry while Fe atoms are octahedrally coordinated. The Ni atoms are coordinated by carbon atoms of four different cyan groups, whereas the Fe atoms are fully coordinated by nitrogen atoms from four different cyan groups and two pyz linkers. Fe[Ni(CN)$_4$] layers are then connected by pyz linkers into a three-dimensional network with one-dimensional channels of about 4.15 × 4.27 or 3.94 × 4.58 Å^2.

[*] Prof. J. Gao, Mr. X. Qian
Institute of Functional Porous Materials, The Key laboratory of Advanced Textile Materials and Manufacturing Technology of Ministry of Education, School of Materials Science and Engineering
Zhejiang Sci-Tech University
Hangzhou 310018 (China)
Email: jkgao@zstu.edu.cn
Prof. J. Gao, Dr. R. -B. Lin, Prof. B. Chen
Department of Chemistry
University of Texas at San Antonio
One UTSA Circle, San Antonio, TX 78249-0698 (USA)
Email: ruibiao.lin@utsa.edu; banglin.chen@utsa.edu
Dr. R. Krishna
Van't Hoff Institute of Molecular Sciences
University of Amsterdam
Science Park 904, 1098 XH Amsterdam (The Netherlands)
Dr. H. Wu, Dr. W. Zhou
NIST Center for Neutron Research
National Institute of Standards and Technology
Gaithersburg, MD 20899-6102 (USA)
Email: wzhou@nist.gov

Supporting information for this article is given via a link at the end of the document.

10.1002/anie.202000323

The open metal sites density of **FeNi-M'MOF** is about 9.2 mmol cm^{-3}, which is higher than that of most MOFs, as shown in Table S2.

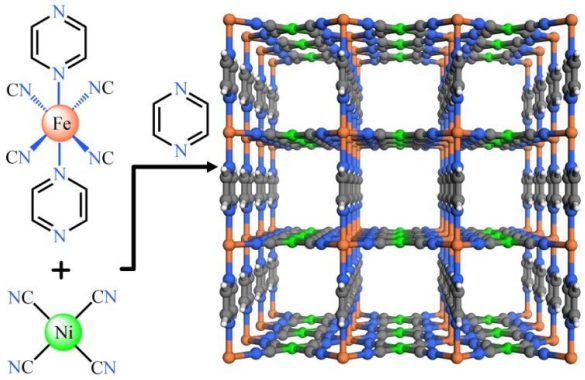

Figure 1. The crystal structure of **FeNi-M'MOF** viewed along the *a/b* axis. Fe, Ni, C, N, H in **FeNi-M'MOF** are represented by orange, green, gray, blue and white, respectively.

FeNi-M'MOF was synthesized at room temperature in water and methanol.[10] By adding the solution of $K_2[Ni(CN)_4]$ into the mixed methanol and water solution of Fe^{2+} and pyz, the **FeNi-M'MOF** microcrystalline powders were obtained after stirring for 30 minutes. The powder X-ray diffraction (PXRD) of products indicated that those products have a good crystallinity and match well with the simulated XRD pattern, indicating the purity of **FeNi-M'MOF**. The resultant **FeNi-M'MOF** was further validated by elemental analysis (EA), thermogravimetry analysis (TGA), energy dispersive spectroscopy (EDS) and X-ray photoelectron spectroscopy (XPS) analysis (see supporting information). This MOF also exhibits an excellent water stability as shown in Figure S2. After soaking in water for 30 days, the crystallinity of **FeNi-M'MOF** is still retained. The TGA curve indicated that **FeNi-M'MOF** exhibits a considerable thermal stability up to 200 ºC (Figure S4). The thermal stability of **FeNi-M'MOF** was also confirmed by variable temperature PXRD (Figure S5), indicating that **FeNi-M'MOF** can maintain its crystalline structure until ~200 ºC. The fast and facile synthesis method, excellent water stability and good thermal stability indicate **FeNi-M'MOF** is a promising separation material for scale-up synthesis.

The Brunauer-Emmett-Teller (BET) surface area of **FeNi-M'MOF** was measured to be 383 $m^2\ g^{-1}$ by N_2 sorption experiment at 77 K as shown in Figure 2a. The experimental total pore volume is ~0.25 $cm^3\ g^{-1}$, and slightly smaller than the theoretical one calculated from the crystal structure (0.30 $cm^3\ g^{-1}$), which can be attributed to the insufficient filling of N_2 molecules in the ultramicroporous pore channels.

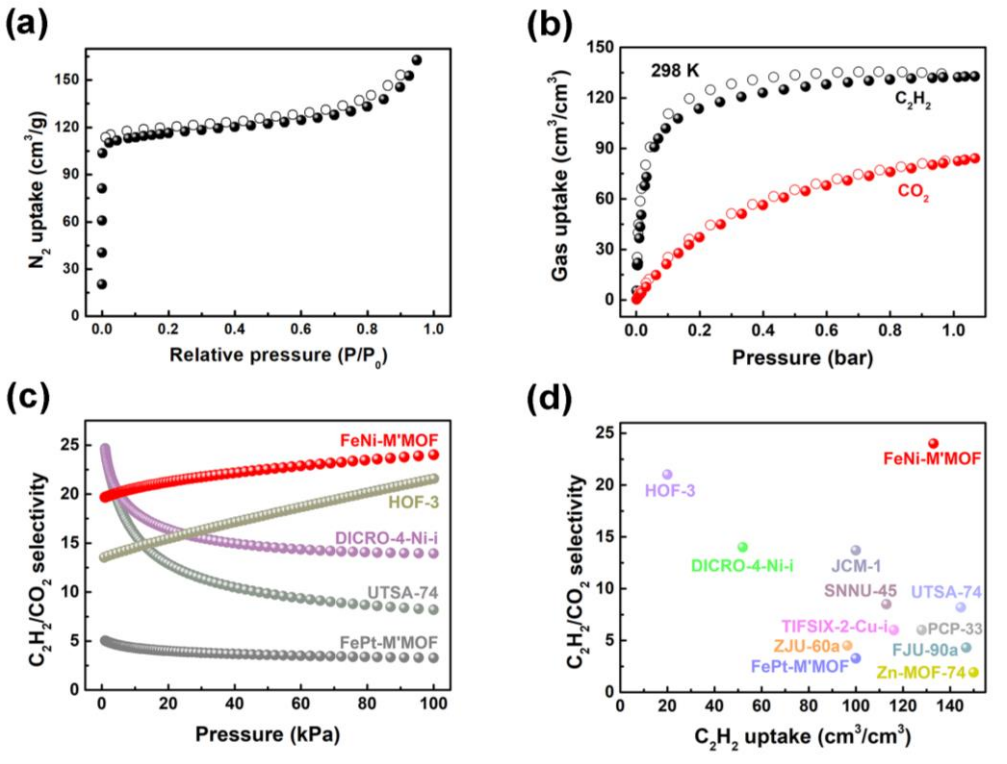

Figure 2. (a) N_2 sorption isotherms for **FeNi-M'MOF** at 77 K. (b) C_2H_2 and CO_2 sorption isotherms for **FeNi-M'MOF** at 298 K. (c) Comparison of IAST selectivities for equimolar C_2H_2/CO_2 mixtures in **FeNi-M'MOF, FePt-M'MOF** and other materials in the range of 0-1 bar at 298 K. (d) Comparison of C_2H_2/CO_2 adsorption selectivity and volumetric C_2H_2 uptake at 1 bar in **FeNi-M'MOF, FePt-M'MOF** and other porous materials.

10.1002/anie.202000323

The C_2H_2 and CO_2 gas adsorption isotherms of **FeNi-M'MOF** were measured at 273 K and 298 K. As shown in Figure 2b, the volumetric C_2H_2 uptake capacity of **FeNi-M'MOF** is 133 cm^3 cm^{-3} (4.29 mmol g^{-1}) at 1 bar and 298 K, which is higher than those of many other MOFs, such as **DICRO-4-Ni-i** (52 cm^3 cm^{-3}),[4e] **ZJU-60a** (96 cm^3 cm^{-3}),[11] Cu[Ni(pdt)$_2$] (108 cm^3 cm^{-3}),[6a] **SNNU-45** (113 cm^3 cm^{-3}),[6b] **TIFSIX-2-Cu-i** (116 cm^3 cm^{-3}),[4f] **PCP-33** (128 cm^3 cm^{-3}),[12] and comparable to those of **UTSA-74** (144 cm^3 cm^{-3}),[5c] **FJU-90a** (146 cm^3 cm^{-3}),[6c] and **Zn-MOF-74** (150 cm^3 cm^{-3})[13]. The CO_2 uptake of **FeNi-M'MOF** is 84 cm^3 cm^{-3} (2.72 mmol g^{-1}) at 1 bar and 298 K. At 1 bar and 273 K, C_2H_2 and CO_2 uptakes of **FeNi-M'MOF** are up to 145 and 102 cm^3 cm^{-3} respectively, as shown in Figure S8. Interestingly, the Pt analogue [Fe(pyz)Pt(CN)$_4$] (**FePt-M'MOF** Figure S10-12) shows much lower uptake capacities for C_2H_2 and CO_2 (100 and 105 cm^3 cm^{-3}, respectively), indicating the potential binding contribution of Ni sites in this type of MOF for C_2H_2 molecules. To evaluate the separation performance of this material, ideal adsorbed solution theory (IAST) was employed to calculate the adsorption selectivity. As shown in Figure 2c, at 100 kPa and 298 K, the C_2H_2/CO_2 (50/50) selectivity of **FeNi-M'MOF** is 24. The selectivity of **FeNi-M'MOF** is higher than those of most MOFs, such as **Zn-MOF-74** (1.92),[5c] **FJU-90a** (4.3),[6c] **UTSA-74a** (8.2),[5c] **JCM-1** (13.4),[4b] **DICRO-4-Ni-i** (13.9),[4e] and benchmark **HOF-3a** (21).[14] It should be noted that both the uptake capacity and separation selectivity can significantly affect the practical performance of an adsorbent. **HOF-3a** has a high selectivity, but the low uptake of C_2H_2 reduced its separation performance. In contrast, **FeNi-M'MOF** can address such trade-off between the adsorption capacity and selectivity as shown in Figure 2d. The high selectivity and high C_2H_2 adsorption capacity of **FeNi-M'MOF** jointly reveal its bright separation potential for C_2H_2/CO_2.

Transient breakthrough simulations were conducted to demonstrate the C_2H_2/CO_2 separation performance of **FeNi-M'MOF**. The simulations in Figure 3a demonstrate the **FeNi-M'MOF** is of potential use for this challenging separation of C_2H_2/CO_2 mixtures. The C_2H_2/CO_2 mixtures (50/50) were used as feeds to mimic the industrial process conditions. Pure CO_2 first eluted through the bed, where the CO_2 purity is 99.95%, and followed by the breakthrough of C_2H_2 after a certain time τ_{break} that **FeNi-M'MOF** has been saturated by C_2H_2. The C_2H_2-captured amount of **FeNi-M'MOF** is 4.54 mol L^{-1} based on the simulated column breakthrough, which is close to that of the benchmark UTSA-74 (4.86 mol L^{-1})[5c] and higher than those of most out-performing MOFs, such as **Zn-MOF-74** (4.06 mol L^{-1}),[5c] **FJU-90a** (4.16 mol L^{-1}),[6c] **PCP-33** (4.16 mol L^{-1})[12]. Accordingly, **FeNi-M'MOF** shows not only a high C_2H_2/CO_2 selectivity and high C_2H_2 uptake but also high C_2H_2-captured capability from gas mixture, enabling this material a huge C_2H_2/CO_2 separation potential. Based on experimental breakthrough studies, we further evaluated the performance of **FeNi-M'MOF** in near practical separation processes for C_2H_2/CO_2 mixture (50/50 v/v) as shown in Figure 3b. Indeed, **FeNi-M'MOF** exhibits excellent C_2H_2/CO_2 mixtures separation performance at 298 K. CO_2 was first eluted through the adsorption bed without any detectable C_2H_2, whereas the latter was retained in the MOF column for a remarkable period prior to saturate the MOF. The retained time of pure CO_2 and C_2H_2 for C_2H_2/CO_2 (50/50 v/v) mixture on **FeNi-M'MOF** are up to 24 and 40 min respectively. Accordingly, the captured-C_2H_2 was calculated to be 4.10 mol L^{-1} with a separation factor of 1.7.

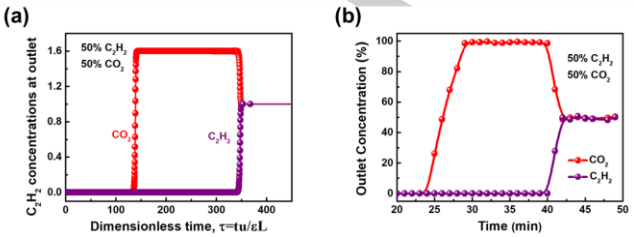

Figure 3. (a) Transient breakthrough simulations for separation of equimolar C_2H_2/CO_2 mixture using **FeNi-M'MOF** at 298 K, with a partial pressure of 50 kPa for each. (b) Experiment breakthrough curves for equimolar C_2H_2/CO_2 mixture in a packed column with **FeNi-M'MOF** at 298 K and 1 bar.

The isosteric heat of adsorption (Q_{st}) has been used to evaluate the strength of interaction between the adsorbent and the adsorbate, which is calculated (Figure S13) from the adsorption isotherms at 273 and 298 K. The Q_{st} values are 27~32.8 and ~24.5 kJ mol^{-1} of **FeNi-M'MOF** for C_2H_2 and CO_2, respectively. The Q_{st} value of C_2H_2 in **FeNi-M'MOF** is lower than those of other MOFs such as **HKUST-1** (39 kJ mol^{-1}),[15] **FeMOF-74** (47.5 kJ mol^{-1}),[16] and **SIFSIX-2-Cu-i** (41.9 kJ mol^{-1}),[1e] and is comparable to that of **UTSA-74** (31 kJ mol^{-1}).[5c] These data indicate **FeNi-M'MOF** has a lower regeneration energy for C_2H_2 production, which would be beneficial for practical application.

To understand the separation performance of **FeNi-M'MOF**, the adsorption modes of C_2H_2 in **FeNi-M'MOF** were established by DFT-D calculations (Figure S14). The modeling structures indicated that there are two binding sites for C_2H_2 in **FeNi-M'MOF**. Site I located in the middle of two adjacent pyz rings, where C_2H_2 was adsorbed through the π-π interactions between C_2H_2 and pyz rings (Figure S14a). The C_2H_2 static binding energy in site I is up to 41.4 kJ mol^{-1}. Site II located in the middle of two adjacent Ni open metal sites, where C_2H_2 molecule was adsorbed through the interactions between C≡C and Ni open metal sites and was perpendicular to *c* axis. The C_2H_2 static binding energy in this site is 29.9 kJ mol^{-1}, which is smaller than that of site I (Figure S14b).

Further visualization of these host-guest interactions was carried out through high-resolution neutron powder diffraction experiments. The crystal structure under low C_2D_2 loading was measured first (Figure 4a). As expected, C_2D_2 molecules preferentially distribute on site I. C_2D_2 molecules were identified between the two pyz rings through π-π stacking (3.552 Å). The C_2D_2 molecules show a titling angle of 27.4º from the [001] direction (crystallographic *c* axis) (Figure S15a). In additional, multiple intermolecular interactions were also observed between C_2D_2 and **FeNi-M'MOF** ($D^{\delta+}\cdots N^{\delta-}$: 2.977 Å, $C^{\delta-}\cdots N^{\delta-}$: 3.808 Å, Figure 4c and Figure S15b). In contrast, the preferential CO_2 binding site is located at the open Ni site (Figure 4b). The electronegative $O^{\delta-}$ atoms of CO_2 interact with the positive open-metal site $Ni^{\delta+}$. However, the distance across the channel is insufficient for favorable $Ni^{\delta+}\cdots O^{\delta-}$=C=$O^{\delta-}\cdots Ni^{\delta+}$ interactions to form in the structure. Thus, CO_2 molecules were adsorbed near the center of the channel and parallel to the channel. $O^{\delta-}$ atom of

10.1002/anie.202000323

CO_2 inserts between the adjacent two $Ni^{\delta+}$ atoms from different layers and the distance of $O^{\delta-}\cdots Ni^{\delta+}$ are 3.746 and 3.325 Å, respectively (Figure 4d). This type interaction is relatively weak, being consistent with the gentle adsorption isotherm and low Q_{st} of CO_2 in **FeNi-M'MOF**. The multiple binding sites of **FeNi-M'MOF** for gas molecules and its different binding modes toward C_2H_2 and CO_2, enable **FeNi-M'MOF** to selective adsorption C_2H_2 from CO_2 with both high C_2H_2 uptake and remarkable C_2H_2/CO_2 selectivity.

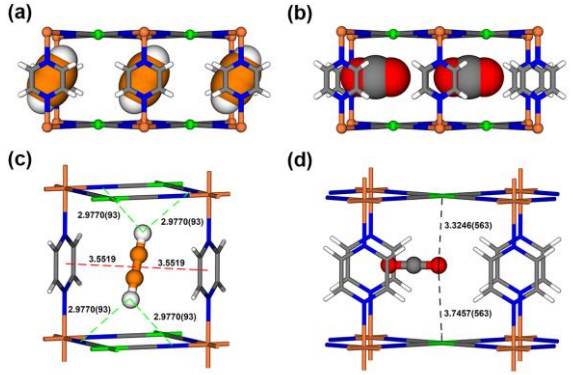

Figure 4. Neutron diffraction crystal structure of **FeNi-M'MOF⊃C_2D_2** (a) and **FeNi-M'MOF⊃CO_2** (b), viewed from *a/b* axis. Adsorption binding sites of C_2D_2 (c) and CO_2 (d) for **FeNi-M'MOF**. Fe, Ni, C, N, O, H in **FeNi-M'MOF** and CO_2 are represented by orange, green, gray, blue, red, and white, respectively; C and D in C_2D_2 are represented by orange and white, respectively. The labelled distance is measured in Å.

In summary, the highly selective C_2H_2/CO_2 separation has been successfully realized by a mixed iron/nickel MOF **FeNi-M'MOF** from metalloligand approach. The structural features of cyanonickelate and optimal pore channels in this MOF allow C_2H_2 molecules to interact on multiple binding sites, with both very high C_2H_2 uptake and C_2H_2/CO_2 selectivity in volumetric ratio. The so-called dual functionality in this material enable this MOFs to serve as one of the best materials for C_2H_2/CO_2 separation in terms of C_2H_2-captured capability. This work also illustrates an outstanding example to further reveal the huge separation potential of MOF adsorbents, especially for challenging gas separation and purification. The active ongoing research affords tremendous opportunities for energy-efficient separation.

Acknowledgements

This work was supported by the Zhejiang Provincial Natural Science Foundation of China (LY20E020001), National Natural Science Foundation of China (51602301 and 51672251) and Welch Foundation (AX-1730). J.G. acknowledges the Fundamental Research Funds of Zhejiang Sci-Tech University (2019Q007).

Conflict of interest

The authors declare no conflict of interest.

Keywords: metal-organic frameworks • gas separation • acetylene • Hofmann • open metal sites

[1] a) H. Li, L. Li, R.-B. Lin, W. Zhou, S. Xiang, B. Chen, Z. Zhang, *EnergyChem* **2019**, *1*, 100006; b) M. Ding, R. W. Flaig, H.-L. Jiang, O. M. Yaghi, *Chem. Soc. Rev.* **2019**, *48*, 2783-2828; c) R.-B. Lin, L. Li, H.-L. Zhou, H. Wu, C. He, S. Li, R. Krishna, J. Li, W. Zhou, B. Chen, *Nat. Mater.* **2018**, *17*, 1128-1133; d) M. K. Taylor, T. Runčevski, J. Oktawiec, J. E. Bachman, R. L. Siegelman, H. Jiang, J. A. Mason, J. D. Tarver, J. R. Long, *J. Am. Chem. Soc.* **2018**, *140*, 10324-10331; e) X. Cui, K. Chen, H. Xing, Q. Yang, R. Krishna, Z. Bao, H. Wu, W. Zhou, X. Dong, Y. Han, B. Li, Q. Ren, M. J. Zaworotko, B. Chen, *Science* **2016**, *353*, 141-144; f) A. Cadiau, K. Adil, P. M. Bhatt, Y. Belmabkhout, M. Eddaoudi, *Science* **2016**, *353*, 137-140; g) R.-B. Lin, S. Xiang, W. Zhou, B. Chen, *Chem* **2019**, DOI: 10.1016/j.chempr.2019.1010.1012.

[2] a) K.-J. Chen, D. G. Madden, S. Mukherjee, T. Pham, K. A. Forrest, A. Kumar, B. Space, J. Kong, Q.-Y. Zhang, M. J. Zaworotko, *Science* **2019**, *366*, 241-246; b) Y. Liu, Z. Chen, G. Liu, Y. Belmabkhout, K. Adil, M. Eddaoudi, W. Koros, *Adv. Mater.* **2019**, *31*, 1807513; c) W. G. Cui, T. L. Hu, X. H. Bu, *Adv. Mater.* **2019**, 1806445; d) R. L. Siegelman, P. J. Milner, E. J. Kim, S. C. Weston, J. R. Long, *Energy Environ. Sci.* **2019**, *12*, 2161-2173; e) L. Li, R.-B. Lin, R. Krishna, H. Li, S. Xiang, H. Wu, J. Li, W. Zhou, B. Chen, *Science* **2018**, *362*, 443-446; f) P.-Q. Liao, N.-Y. Huang, W.-X. Zhang, J.-P. Zhang, X.-M. Chen, *Science* **2017**, *356*, 1193-1196; g) S. Yang, A. J. Ramirez-Cuesta, R. Newby, V. Garcia-Sakai, P. Manuel, S. K. Callear, S. I. Campbell, C. C. Tang, M. Schröder, *Nat. Chem.* **2014**, *7*, 121-129; h) M. L. Aubrey, M. T. Kapelewski, J. F. Melville, J. Oktawiec, D. Presti, L. Gagliardi, J. R. Long, *J. Am. Chem. Soc.* **2019**, *141*, 5005-5013.

[3] C. R. Reid, K. M. Thomas, *J. Phys. Chem. B* **2001**, *105*, 10619-10629.

[4] a) H. Yang, T. X. Trieu, X. Zhao, Y. Wang, Y. Wang, P. Feng, X. Bu, *Angew. Chem. Int. Ed.* **2019**, *58*, 11757-11762; b) J. Lee, C. Y. Chuah, J. Kim, Y. Kim, N. Ko, Y. Seo, K. Kim, T. H. Bae, E. Lee, *Angew. Chem. Int. Ed.* **2018**, *57*, 7869-7873; c) R.-B. Lin, L. Li, H. Wu, H. Arman, B. Li, R.-G. Lin, W. Zhou, B. Chen, *J. Am. Chem. Soc.* **2017**, *139*, 8022-8028; d) M. Jiang, X. Cui, L. Yang, Q. Yang, Z. Zhang, Y. Yang, H. Xing, *Chem. Eng. J.* **2018**, *352*, 803-810; e) H. S. Scott, M. Shivanna, A. Bajpai, D. G. Madden, K.-J. Chen, T. Pham, K. A. Forrest, A. Hogan, B. Space, J. J. Perry Iv, M. J. Zaworotko, *ACS Appl. Mater. Interfaces* **2017**, *9*, 33395-33400; f) K.-J. Chen, H. S. Scott, D. G. Madden, T. Pham, A. Kumar, A. Bajpai, M. Lusi, K. A. Forrest, B. Space, J. J. Perry IV, Michael J. Zaworotko, *Chem* **2016**, *1*, 753-765; g) O. T. Qazvini, R. Babarao, Z.-L. Shi, Y.-B. Zhang, S. G. Telfer, *J. Am. Chem. Soc.* **2019**, *141*, 5014-5020.

[5] a) H. Zeng, M. Xie, Y.-L. Huang, Y. Zhao, X.-J. Xie, J.-P. Bai, M.-Y. Wan, R. Krishna, W. Lu, D. Li, *Angew. Chem. Int. Ed.* **2019**, *58*, 8515-8519; b) J. Duan, M. Higuchi, J. Zheng, S.-I. Noro, I.-Y. Chang, K. Hyeon-Deuk, S. Mathew, S. Kusaka, E. Sivaniah, R. Matsuda, *J. Am. Chem. Soc.* **2017**, *139*, 11576-11583; c) F. Luo, C. Yan, L. Dang, R. Krishna, W. Zhou, H. Wu, X. Dong, Y. Han, T.-L. Hu, M. O'Keeffe, L. Wang, M. Luo, R.-B. Lin, B. Chen, *J. Am. Chem. Soc.* **2016**, *138*, 5678-5684.

[6] a) Y.-L. Peng, T. Pham, P. Li, T. Wang, Y. Chen, K.-J. Chen, K. A. Forrest, B. Space, P. Cheng, M. J. Zaworotko, Z. Zhang, *Angew. Chem. Int. Ed.* **2018**, *57*, 10971-10975; b) Y.-P. Li, Y. Wang, Y.-Y. Xue, H.-P. Li, Q.-G. Zhai, S.-N. Li, Y.-C. Jiang, M.-C. Hu, X. Bu, *Angew. Chem. Int. Ed.* **2019**, *58*, 13590-13595; c) Y. Ye, Z. Ma, R.-B. Lin, R. Krishna, W. Zhou, Q. Lin, Z. Zhang, S. Xiang, B. Chen, *J. Am. Chem. Soc.* **2019**, *141*, 4130-4136.

[7] a) D. Aguila, Y. Prado, E. S. Koumousi, C. Mathoniere, R. Clérac, *Chem. Soc. Rev.* **2016**, *45*, 203-224; b) M. B. Zakaria, T. Chikyow, *Coord. Chem. Rev.* **2017**, *352*, 328-345; c) K. Otsubo, T. Haraguchi, H. Kitagawa, *Coord. Chem. Rev.* **2017**, *346*, 123-138; d) S. Sakaida, K. Otsubo, O. Sakata, C. Song, A. Fujiwara, M. Takata, H. Kitagawa, *Nat. Chem.* **2016**, *8*, 377-383; e) M. M. Deshmukh, M. Ohba, S. Kitagawa, S. Sakaki, *J. Am. Chem. Soc.* **2013**, *135*, 4840-4849; f) J. T. Culp, M. R. Smith, E. Bittner, B. Bockrath, *J. Am. Chem. Soc.* **2008**, *130*, 12427-12434.

[8] a) M. C. Das, S. Xiang, Z. Zhang, B. Chen, *Angew. Chem. Int. Ed.* **2011**, *50*, 10510-10520; b) S.-C. Xiang, Z. Zhang, C.-G. Zhao, K. Hong, X. Zhao, D.-R. Ding, M.-H. Xie, C.-D. Wu, M. C. Das, R. Gill, K. Tomas, B. Chen, *Nat. Commun.* **2011**, *2*, 204.

[9] V. Niel, J. M. Martinez-Agudo, M. C. Muñoz, A. B. Gaspar, J. A. Real, *Inorg. Chem.* **2001**, *40*, 3838-3839.

[10] J. Gao, J. Cong, Y. Wu, L. Sun, J. Yao, B. Chen, *ACS Appl. Energy Mater.* **2018**, *1*, 5140-5144.

[11] X. Duan, Q. Zhang, J. Cai, Y. Yang, Y. Cui, Y. He, C. Wu, R. Krishna, B. Chen, G. Qian, *J. Mater. Chem. A* **2014**, *2*, 2628-2633.

[12] J. Duan, W. Jin, R. Krishna, *Inorg. Chem.* **2015**, *54*, 4279-4284.

10.1002/anie.202000323

[13] S. Xiang, W. Zhou, Z. Zhang, M. A. Green, Y. Liu, B. Chen, *Angew. Chem. Int. Ed.* **2010**, *49*, 4615-4618.
[14] P. Li, Y. He, Y. Zhao, L. Weng, H. Wang, R. Krishna, H. Wu, W. Zhou, M. O'Keeffe, Y. Han, B. Chen, *Angew. Chem. Int. Ed.* **2015**, *54*, 574-577.
[15] Y. He, R. Krishna, B. Chen, *Energy Environ. Sci.* **2012**, *5*, 9107-9120.
[16] E. D. Bloch, W. L. Queen, R. Krishna, J. M. Zadrozny, C. M. Brown, J. R. Long, *Science* **2012**, *335*, 1606-1610.

10.1002/anie.202000323

WILEY-VCH

Entry for the Table of Contents

COMMUNICATION

FeNi-M'MOF with a microporous one-dimensional channel decorated with multiple binding sites shows a high C_2H_2 uptake (133 cm^3 cm^{-3}) and high C_2H_2/CO_2 selectivity (24).

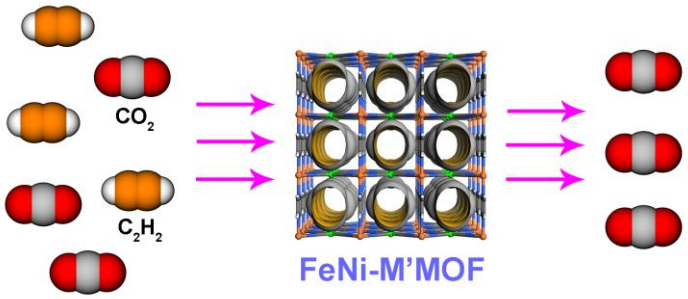

J. Gao, X. Qian, R.-B. Lin*, R. Krishna, H. Wu, W. Zhou*, B. Chen**

Page No. – Page No.

Mixed Metal-Organic Framework with Multiple Binding Sites for Efficient C_2H_2/CO_2 Separation